Biodegradable Polyesters as Crystallization-Accelerating Agents of Poly(L-lactide)

Hideto Tsuji,* Mariko Sawada, and Leevameng Bouapao

Department of Ecological Engineering, Faculty of Engineering, Toyohashi University of Technology, Tempaku-cho, Toyohashi, Aichi 441-8580, Japan

ABSTRACT A series of biodegradable polyesters, poly[(R)-3-hydroxybutyrate] (PHB), poly(ϵ-caprolactone) (PCL), and polyglycolide (PGA), were found to be effective crystallization-accelerating agents for poly(L-lactide) (PLLA). Differential scanning calorimetry and polarized optical microscopy strongly suggested that the accelerated crystallization of PLLA in the presence of the three biodegradable polyesters is attributable to a nucleation-assisting effect of PCL and PGA and a spherulite growth-accelerating effect of PHB, although the incorporated PHB lowered the spherulite number of PLLA per unit area. The spherulite growth-accelerating effect of PHB probably resulted from the relatively high miscibility of PLLA with PHB and the low glass transition temperature of PHB compared to that of PLLA. The crystallization kinetics of PLLA varied only in the case of PLLA/PHB blends during cooling from the melt, as evidenced by the nucleation constant and radius growth rate values of the spherulites. The nucleation and growth types of PLLA crystallites are thought to be altered only in the case of PLLA/PGA blends during heating, as evidenced by Avrami exponent n values.

KEYWORDS: biodegradable polyesters • crystallization • nucleation • poly(L-lactic acid)

INTRODUCTION

Poly(L-lactide), i.e., poly(L-lactic acid) (PLLA), is a plant-derived polyester and is widely used as an alternative material to petro-derived polymers. The enhancement of the thermal stability or heat resistance of PLLA is a crucial issue in widening the scope of industrial and commodity applications (1−15). Numerous studies have been carried out for improving the thermal stability of PLLA. One of the most effective methods is to elevate its crystallinity by the addition of inorganic nucleating agents, such as talc, montmorillonite, and nanostructured carbon (16−29), and of low-molecular-weight organic compounds, such as amide and hydrazide (29, 30). Recently, an attempt was carried out to utilize the stereocomplex of PLLA/poly(D-lactide), i.e., poly(D-lactic acid) (PDLA), as a biodegradable nucleating agent for PLLA (18, 23, 32−35).

The properties, processability, and production rate (cost) of PLLA articles depend on the crystallization behavior, rate, and final crystallinity. Increasing the crystallization rate is crucial to elevating the production rate (i.e., reducing the production cost) and elevating the heat resistance of the final products. However, too high a crystallization rate can cause difficulty in the secondary processing of preformed PLLA articles. Therefore, various types of nucleating agents or crystallization-manipulating agents are required to optimize the crystallization behavior and rate in the industrial processing of PLLA. The use of biodegradable nucleating or crystallization-manipulating agents, like biodegradable poly-esters, facilitates the design and preparation of totally biodegradable materials, which can be used for biomedical and environmental applications having various physical properties and biodegradability.

A previous study indicated that polyglycolide, i.e., poly(glycolic acid) (PGA), with a melting temperature (220−230 °C) much higher than that of PLLA (170−180 °C), can act as a crystallization-accelerating agent for PLLA, even at a PGA content as low as 0.1 wt % (36). This study suggested that the accelerating mechanism of PGA is rather different from that of reported inorganic nucleating agents and the PLLA/PDLA stereocomplex. On the other hand, the addition of biodegradable polyesters, such as poly(ϵ-caprolactone) (PCL) and poly[(R)-3-hydroxybutyrate] (PHB), has been frequently studied to modify the mechanical performance of PLLA or poly(DL-lactide), i.e., poly(DL-lactic acid) (PDLLA). From these studies, PLLA is found to crystallize in the presence of PCL up to 80 or 90 wt % (37, 38) and of PHB up to 70 or 75 wt % (39−42). PLLA is immiscible with PCL (37, 38), whereas low-molecular-weight PLLA is miscible with PHB, but the miscibility becomes lower with an increase in the molecular weight of either polymer (39−41). Investigation of the crystallization behavior and rate of PLLA in the presence of biodegradable polyesters as additives at contents below 10 wt % is expected to give useful information regarding optimization of the crystallization behavior and rate of PLLA. However, as far as we are aware, despite intensive study of the crystallization of PLA-based polymer blends, there have been few reports on this issue.

The objectives of the present study were to investigate the effectiveness of biodegradable polyesters as crystalliza-tion-accelerating agents for PLLA and to compare the ac-

Table 1. Thermal Properties of Melt-Quenched Pure PLLA and Other Biodegradable Polyesters and Their Blends during Heating from Room Temperature (Process I)

| base polymer | incorporated polyester | | casting solvent[a] | $T_g{}^b$ (°C) | $T_{cc}(S)^c$ (°C) | $T_{cc}(P)^c$ (°C) | $T_{cc}(F)^c$ (°C) | $T_m{}^d$ (°C) | $\Delta H_{cc}{}^e$ (J g^{-1}) | $\Delta H_m{}^e$ (J g^{-1}) |
	type	content (wt %)								
PLLA	not added	0	C	56.5	107.7	129.7	151.0	163.7	−24.4	24.2
			H	57.4	112.1	136.8	153.7	164.6	−10.0	11.2
	PHB	10	C	57.4	107.0	128.5	150.4	164.0	−21.3	22.9
	PCL		C	55.8[f]	103.3	113.7	127.8	162.0, 166.6	−28.2	29.2
	PGA		H	57.7	107.5	114.6	122.7	161.2, 166.4	−29.5	29.5
	PHB	1	C	57.5	107.9	128.1	151.7	164.2	−20.7	21.4
PHB	not added	0	C		35.5	46.0	52.1	175.1	−21.6	89.8
PCL	not added	0	C					55.2	0	67.6
PGA	not added	0	H	35.4				206.1, 221.3	0	62.0

[a] C and H mean chloroform and HF2P, respectively. [b] Glass transition temperature. [c] $T_{cc}(S)$, $T_{cc}(P)$, and $T_{cc}(F)$ are the starting, peak, and final temperatures of cold crystallization. [d] Melting temperature. [e] ΔH_{cc} and ΔH_m are the enthalpies of cold crystallization and melting. [f] Melting temperature of PCL, not the glass transition temperature of blend.

celerating mechanisms of the biodegradable polyesters with those of the reported nucleating agents. For these purposes, the crystallization of PLLA in the presence of representative biodegradable polyesters (PCL, PHB, and PGA) at contents below 10% was investigated by differential scanning calorimetry (DSC) and polarized optical microscopy (POM), and their crystallization-accelerating mechanisms are discussed based on the obtained results.

EXPERIMENTAL SECTION

Materials. PLLA was kindly supplied by Unitika Co. (Kyoto, Japan) and was purified by previously reported methods (23, 24, 27). The purified PLLA [number-average molecular weight (M_n) = 9.5×10^4, weight-average molecular weight (M_w)/M_n = 1.9, specific optical rotation in chloroform ([α]$^{25}_{589}$) = −141° dm^{-1} g^{-1} cm^3] was dried in vacuo for at least 7 days. PCL ($M_n \sim 8 \times 10^4$ g mol^{-1}), PHB (natural origin), and PGA (inherent viscosity = 1.4−1.8 dL g^{-1}) were purchased from Sigma-Aldrich Co. (St. Louis, MO). PGA was used as received, whereas PHB and PCL were purified with the precipitation method reported earlier (43). The M_n and M_w/M_n values of purified PHB were 3.0×10^5 g mol^{-1} and 2.3, respectively, and those of purified PCL were 1.1×10^5 g mol^{-1} and 1.6, respectively). Blends (40−50 μm thick) with different biodegradable polyester contents were prepared by the following procedures. For the preparation of PLLA/PHB and PLLA/PCL blends, mixtures of PLLA/PHB and PLLA/PCL were simultaneously dissolved in chloroform. For the preparation of PLLA/PGA blends, PGA was dissolved in 1,1,1,3,3,3-hexafluoro-2-propanol (abbreviated as HF2P, special grade for HPLC, Nacalai Tesque, Inc., Kyoto, Japan) at 70 °C, and then PLLA was dissolved in the PGA solution at room temperature (36). The thus-prepared solutions (1 g of polymers dL^{-1}) were cast onto Petri dishes, and then the solvent was allowed to evaporate at 25 °C for approximately 2 days, but in the case of PLLA/PGA blends, HF2P cannot be completely removed only by evaporation, so the solvent remaining in the obtained films was extracted with methanol at 25 °C for 5 h and then dried in vacuo for at least 7 days. Methanol was replaced once after 1 h of extraction. To discriminate between the pure PLLA films prepared with chloroform and HF2P (as blank specimens of PLLA/PHB and PLLA/PCL blends and of PLLA/PGA blends, respectively), these films are abbreviated as PLLA(C) and PLLA(H), respectively. Also, the figure in parentheses after the blend expression is the content of the biodegradable polymer. For example, "PLLA/PHB(10)" means that the PLLA/PHB blend contains 10 wt % PHB.

Measurements and Observation. Crystallization of the specimens (sample weight ca. 3 mg) was monitored during heating and cooling using a Shimadzu (Kyoto, Japan) DSC-50 differential scanning calorimeter under a nitrogen gas flow. For monitoring of the crystallization during heating, melt-quenched specimens, which were prepared by heating as-cast films at a rate of 10 °C min^{-1} from room temperature to 200 °C and then quenching at room temperature, were again heated at a rate of 10 °C min^{-1} from room temperature to 200 °C (process I: crystallization was observed here). For tracing of the crystallization during cooling from the melt, the as-cast films were heated at a rate of 10 °C min^{-1} from room temperature to 200 °C, held at the same temperature for 3 min, and then cooled at a rate of −1 °C min^{-1} (process II: crystallization was observed here). The crystallinity of PLLA in the specimens (X_c) after completion of crystallization was evaluated according to the following equation:

$$X_c (\%) = 100(-\Delta H_{cc})/[135(1 - X_{BP}/100)] \quad (1)$$

where ΔH_{cc} is the enthalpy of cold crystallization of PLLA, 135 J g^{-1} is the enthalpy of melting of PLLA crystals having an infinite size (44), and X_{BP} is the biodegradable polyester (PCL, PHB, or PGA) weight fraction (wt %) in the specimen. By definition, ΔH_{cc} is negative. The thermal properties of pure PLLA, PHB, PCL, and PGA during heating from room temperature (process I) are shown in Table 1. It is evident from this table that PCL and PGA will not give any peaks in the PLLA crystallization temperature range of 80−160 °C, whereas PHB is reported not to crystallize in the presence of PLLA when the PHB content was lowered to 20 wt % (39). In our previous study, it was confirmed that the deviation values from the averaged ones for the glass transition, cold crystallization, and melting temperatures (T_g, T_{cc}, and T_m) and ΔH_{cc} were below 0.5 °C and 1 J g^{-1}, respectively. We carried out duplicate or triplicate measurements when the thermal values showed an irregular dependence on the biodegradable polyester content and confirmed that the trend is not based on experimental errors.

Spherulite growth in the films was observed during processes II and III using an Olympus (Tokyo, Japan) polarization optical microscope (BX50) equipped with a heating−cooling stage and a temperature controller (LK-600PM, Linkam Scientific Instruments, Surrey, U.K.) under a constant nitrogen gas flow. The as-cast films were first heated at a rate of 100 °C min^{-1} from room temperature to 200 °C, held at the same temperature for 3 min, cooled at −1 °C min^{-1} (process II, spherulite growth was observed here for nonisothermal crystallization) or cooled at a
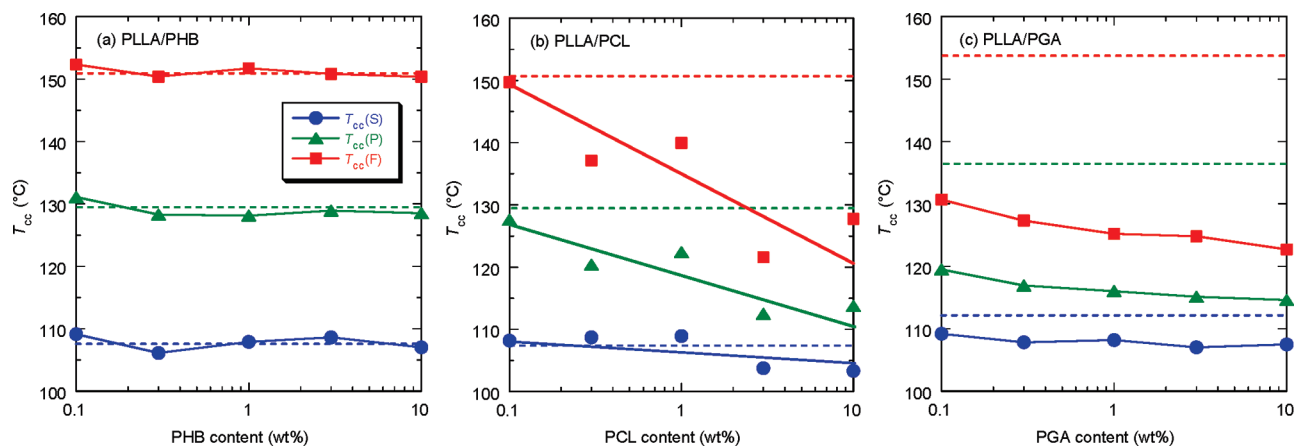
FIGURE 1. Starting, peak, and final temperatures of cold crystallization [$T_{cc}(S)$, $T_{cc}(P)$, and $T_{cc}(F)$, respectively] of melt-quenched PLLA/PHB (a), PLLA/PCL (b), and PLLA/PGA (c) blends during heating from room temperature (process I) as a function of the biodegradable polyester content. The broken lines show the values for pure PLLA, i.e., at biodegradable polyester content of 0 wt %: (a and b) PLLA(C); (c) PLLA(H).

rate of −100 °C min⁻¹ to crystallization temperature (T_c) of 110 or 130 °C, and held at the same T_c (process III; spherulite growth was observed here for isothermal crystallization).

RESULTS

DSC. The glass transition, cold crystallization, and melting peaks of PLLA were observed at around 60, 120, and 170 °C on DSC thermograms of melt-quenched PLLA/PHB, PLLA/PCL, and PLLA/PGA blends during heating from room temperature (process I; Figure S1 in the Supporting Information). The relatively sharp endothermic peak of PLLA/PCL(10) (i.e., a PLLA/PCL blend with 10 wt % PCL) observed at 60 °C is ascribed to the melting of PCL. The starting, peak, and final temperatures of cold crystallization [$T_{cc}(S)$, $T_{cc}(P)$, and $T_{cc}(F)$, respectively] were estimated from the DSC thermograms (Figure S1 in the Supporting Information) and are plotted in Figure 1 as functions of the biodegradable polyester content. Here, $T_{cc}(P)$ is the peak temperature of cold crystallization, whereas $T_{cc}(S)$ and $T_{cc}(F)$ are the intersection temperatures of the baseline and the tangent lines for cold crystallization curves lower and higher than $T_{cc}(P)$, respectively, as is schematically illustrated in the reported literature (23, 24, 27). The thermal properties of pure PLLA, other biodegradable polyesters, and their blends are summarized in Table 1.

The differences in the $T_{cc}(S)$, $T_{cc}(P)$, and $T_{cc}(F)$ values of PLLA(C), i.e., pure PLLA prepared with chloroform (at 0 wt % PLLA/PHB and PLLA/PCL blends), and those of PLLA(H), i.e., pure PLLA prepared with HF2P (at 0 wt % PLLA/PGA blends), may be attributed to the effect of the solvent type. Probably, crystallization during solvent evaporation was affected by the solvent type, and the effect of the solvent-evaporation-formed structure remained even after melting, affecting the T_{cc} values during heating. The $T_{cc}(S)$, $T_{cc}(P)$, and $T_{cc}(F)$ of PLLA/PHB blends remained unvaried, regardless of the PHB content. In contrast, $T_{cc}(S)$ of the PLLA/PCL blends became lower when the PCL content was increased over 1 wt %, whereas $T_{cc}(P)$ and $T_{cc}(F)$ of the PLLA/PCL blends decreased gradually with an increase in the PCL content. On the other hand, $T_{cc}(S)$ of the PLLA/PGA blends gradually decreased with an increase in the PGA content, whereas

$T_{cc}(P)$ and $T_{cc}(F)$ decreased dramatically when the PGA content was increased from 0 to 0.1 wt % and then slowly decreased when the PGA content was elevated from 0.1 to 10 wt %. It is surprising that even the addition of 0.1 wt % PGA significantly decreased the $T_{cc}(S)$, $T_{cc}(P)$, and $T_{cc}(F)$ values by 3, 17, and 23 °C, respectively.

The X_c values of melt-quenched PLLA/PCL, PLLA/PHB, and PLLA/PGA blends after the completion of crystallization during heating (process I) were estimated from the DSC thermograms (Figure S1 in the Supporting Information) and are plotted in Figure 2 as functions of the biodegradable polyester content. The difference in the X_c values of pure PLLA at 0 wt % PLLA/PHB and PLLA/PCL blends [i.e., PLLA(C)] and PLLA/PGA blends [i.e., PLLA(H)] prepared respectively with chloroform and HF2P can be ascribed to the aforementioned reason. Before thermal treatment, the X_c value of as-cast PLLA(C) (11.0%) was lower than that (24.9%) of as-cast PLLA(H). This suggests that the initial X_c values before thermal treatment are not directly related to the X_c values after thermal treatment. The X_c values of PLLA/PHB blends were slightly lower or the same as that of PLLA(C), whereas those of PLLA/PCL blends increased gradually with an increase in the PCL content. Similar to the trend of the $T_{cc}(P)$ and $T_{cc}(F)$ values, the X_c values of PLLA/PGA blends dramatically increased from 7.4 to 26.5% when the PGA content was increased from 0 to 0.1 wt % but remained practically constant at around 25% for a PGA content range of 0.1−10 wt %.

DSC thermograms of as-cast PLLA/PCL, PLLA/PHB, and PLLA/PGA blends during cooling from the melt (process II) showed only the crystallization peaks of PLLA (Figure S2 in the Supporting Information). The $T_{cc}(S)$, $T_{cc}(P)$, and $T_{cc}(F)$ values were estimated from the DSC thermograms (Figure S2 in the Supporting Information) according to the aforementioned procedure, although $T_{cc}(S)$ and $T_{cc}(F)$ are the intersection temperatures of the baseline and the tangent lines for crystallization curves higher and lower than $T_{cc}(P)$, respectively (22, 23, 26). The thus-obtained T_{cc} values are plotted in Figure 3 as functions of the biodegradable polyester content. The $T_{cc}(S)$, $T_{cc}(P)$, and $T_{cc}(F)$ values of PLLA/
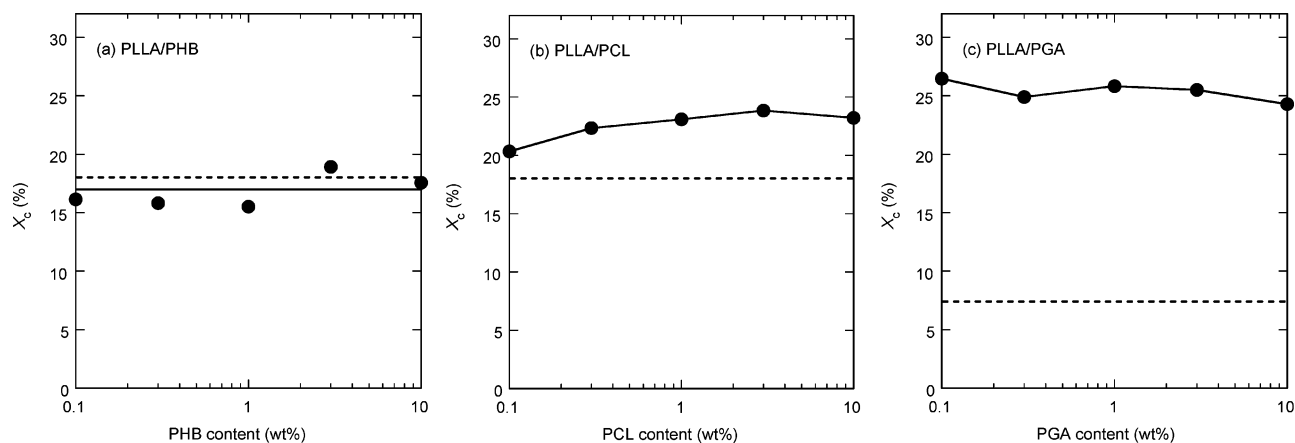
FIGURE 2. Crystallinity (X_c) of melt-quenched PLLA/PHB (a), PLLA/PCL (b), and PLLA/PGA (c) blends after cold crystallization during heating from room temperature (process I) as a function of the biodegradable polyester content. The broken lines show the values for pure PLLA, i.e., at biodegradable polyester content of 0 wt %: (a and b) PLLA(C); (c) PLLA(H).
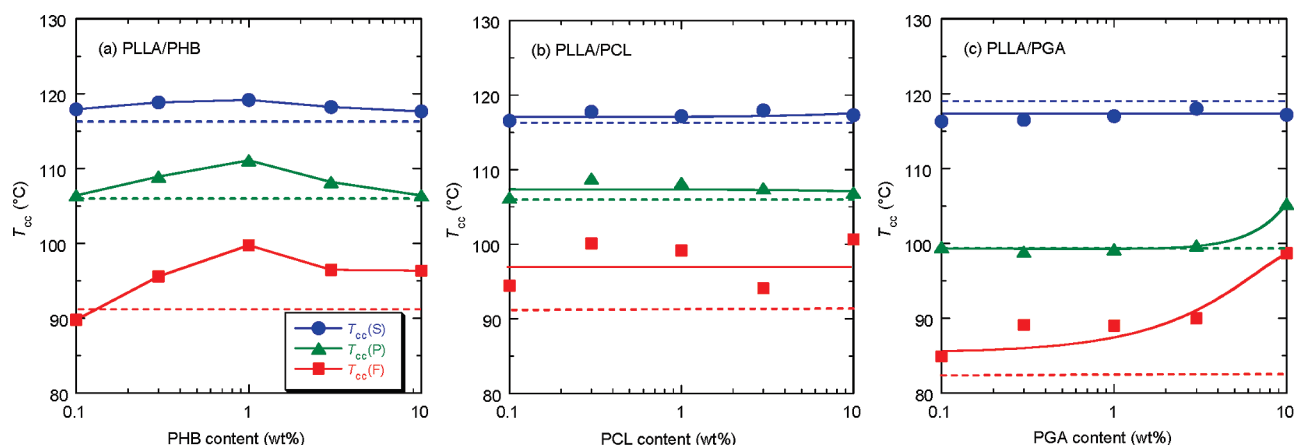

FIGURE 3. $T_{cc}(S)$, $T_{cc}(P)$, and $T_{cc}(F)$ of as-cast PLLA/PHB (a), PLLA/PCL (b), and PLLA/PGA (c) blends during cooling from the melt (process II) as a function of the biodegradable polyester content. The broken lines show the values for pure PLLA, i.e., at biodegradable polyester content of 0 wt %: (a and b) PLLA(C); (c) PLLA(H).

PHB blends, excluding the $T_{cc}(S)$, $T_{cc}(P)$, and $T_{cc}(F)$ values at 0.1 wt % and the $T_{cc}(S)$ and $T_{cc}(P)$ values at 10 wt %, were higher than those of pure PLLA and gave maxima at 1 wt %. In contrast, the incorporated PCL and PGA had no significant effect on the $T_{cc}(S)$ and $T_{cc}(P)$ values, except for the $T_{cc}(P)$ value of the PLLA/PGA(10) blend, although the $T_{cc}(S)$ and $T_{cc}(P)$ values of PLLA/PCL blends and the $T_{cc}(S)$ values of PLLA/PGA blends were respectively slightly higher and lower than those of pure PLLA. On the other hand, the $T_{cc}(F)$ values of PLLA/PCL and PLLA/PGA blends were higher than that of pure PLLA. The $T_{cc}(F)$ values of PLLA/PCL blends are independent of the PCL content range of 0.1−10 wt %, whereas the $T_{cc}(F)$ values of PLLA/PGA blends increased with an increase in the PGA content. In summary, at least the $T_{cc}(F)$ values of the blends, excluding that of the PLLA/PHB(0.1) blend, were significantly increased by the incorporated biodegradable polyesters.

The X_c values of as-cast PLLA/PCL, PLLA/PHB, and PLLA/PGA blends after the completion of crystallization during cooling from the melt were estimated from the DSC thermograms (Figure S2 in the Supporting Information) and are plotted in Figure 4 as functions of the biodegradable polyester content. Most of the X_c values, excluding that of the PLLA/PHB(3) blend, were higher than those of pure PLLA.

The X_c values of the PLLA/PCL blends increased with an increase in the PCL content up to 0.3 wt %, and then the values were stabilized for the PCL content range of 0.3−10 wt %. The X_c values of PLLA/PGA blends increased gradually with an increase in the PGA content. The dramatic increase in X_c of PLLA during the heating process upon the addition of PGA was not observed in the cooling process. In contrast, the X_c values of PLLA/PHB blends increased significantly only when the PHB content was elevated to 10 wt %.

POM. The effects of the incorporated biodegradable polyesters on the spherulite growth behavior of PLLA were further investigated by the use of POM. Figure 5 shows the polarized optical photomicrographs of pure PLLA and PLLA/PCL, PLLA/PHB, and PLLA/PGA blends taken during cooling from the melt (process II). Here, because of the fact that the incorporated PHB increased the radius growth rate (G) of PLLA sperulties, the effects of the PHB content were investigated only for PLLA/PHB blends. As seen in Figure 5, the spherulites of pure PLLA and its blends started to be formed at 130 °C and their growth was completed at 90 °C. The area covered with spherulites at 110 °C was higher for the blends than for pure PLLA; PLLA/PCL(10) (50%) ≅ PLLA/PHB(1) (51%) > PLLA/PHB(10) (45%) > PLLA(C) (32%);

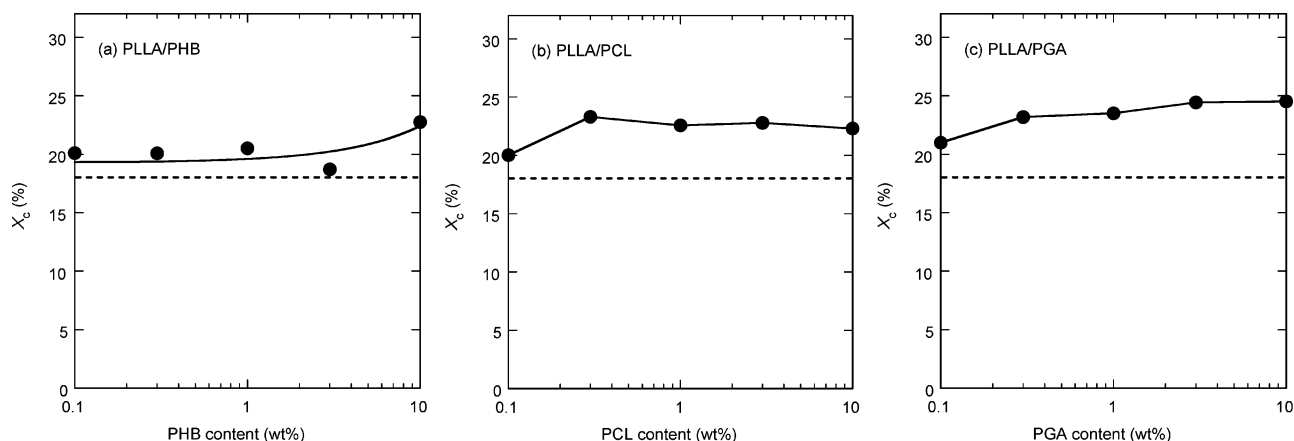**FIGURE 4.** X_c of as-cast PLLA/PHB (a), PLLA/PCL (b), and PLLA/PGA (c) blends during cooling from the melt (process II) as a function of the biodegradable polyester content. The broken lines show the values for pure PLLA, i.e., at biodegradable polyester content of 0 wt %: (a) and (b) PLLA(C); (c) PLLA(H).

PLLA/PGA(10) (96 %) > PLLA(H) (62 %). This supports the DSC result that incorporated biodegradable polyesters accelerated the overall crystallization rate. The final spherulite size at 90 °C decreased in the following order: PLLA/PHB(10) > PLLA/PHB(1) ≅ PLLA(C) > PLLA/PCL(10); PLLA(H) > PLLA/PGA(10). This result reflects the fact that the incorporated PCL and PGA increased the nucleus number of PLLA spherulites, whereas the incorporated PHB lowered the nucleus number of PLLA spherulites when the PHB content was increased to as high as 10 wt %. The rather distorted Maltese crosses but no concentric extinctions along the radius direction were observed in the spherulites, irrespective of the presence or absence of biodegradable polyesters and of the types and concentrations of biodegradable polyesters. The former reflects the disordered orientation of PLLA lamellae, whereas the latter means that the rotation of the lamellae is nonperiodical.

For evaluation of the spherulite growth, the R values of the blends during cooling from the melt (process II) are plotted in Figure 6 as a function of the crystallization temperature (T_c). The averaged G (G_{av}) and the onset temperature of cold crystallization for spherulite growth [T_{cc}(O)] were estimated assuming that spherulite growth takes place linearly with time, independent of T_c (Figure 6). The obtained G_{av} and T_{cc}(O) are tabulated in Table 2. The G_{av} values of PLLA/PHB(10) and PHB(1) blends were respectively significantly and slightly higher than those of pure PLLA, PLLA/PCL(10), and PLLA/PGA(10), reflecting the fact that the incorporated PHB can elevate G_{av}. The T_{cc}(O) of PLLA/PHB(10) (133 °C) was significantly lower than those of pure PLLA (141 and 142 °C), PLLA/PHB(1) (139 °C), PLLA/PCL(10) (141 °C), and PLLA/PGA(10) (140 °C). This indicates that too high a concentration of incorporated PHB can disturbed the formation of PLLA spherulite nuclei and, therefore, increase the final size of PLLA spherulites in PLLA/PHB(10) after the completion of crystallization, as observed at 90 °C in Figure 5.

The G values were estimated for each T_c from the R values in Figure 6, according to the method utilized by Di Lorenzo (45) and the thus-obtained G values of pure PLLA and the blends were plotted in Figure 7 as a function of T_c. As seen in Figure 7, the incorporated PCL and PGA did not alter the G values. In marked contrast, the incorporated PHB largely and slightly increased the G values at some T_c values in PLLA/PHB(10) and PLLA/PHB(1) blends, respectively. To confirm the validity of the G values obtained in nonisothermal measurements and to estimate the induction period for PLLA spherulite growth (t_i), we carried out isothermal observation with a polarized optical microscope (process III). Here, the G values were estimated from the slope of the spherulite radii against crystallization time, whereas the t_i values were evaluated from extrapolation of the spherulite radius plotted against the crystallization time to a radius of 0 μm. The G values obtained from the isothermal experiments (Table S1 in the Supporting Information) were similar to those obtained by the nonisothermal experiments (process II) and, therefore, validate the result of nonisothermal experiments that the incorporated PHB largely and slightly increased G values in PLLA/PHB(10) and PLLA/PHB(1) blends, respectively, whereas the incorporated PCL and PGA did not alter the G values of PLLA. However, the t_i values in the isothermal experiments remained unchanged in the presence of PHB, PCL, and PGA (Table S1 in the Supporting Information), consistent with very small changes in the T_{cc}(S) values in the nonisothermal experiments in the presence of these biodegradable polyesters. Again, a large increase in the number of PLLA spherulites was observed in the presence of PGA in the isothermal experiments (Table S1 in the Supporting Information), in agreement with the results in the nonisothermal experiments.

Hoffman Analysis. In order to elucidate the crystallization kinetics, we estimated the nucleation constant (K_g) and the front constant (G_0) of the specimens by use of the nucleation theory established by Hoffman et al. (46, 47), in which G can be expressed by the following equation:

$$G = G_0 \exp[-U^*/R(T_c - T_\infty)] \exp[-K_g/(T_c \Delta T f)]$$

(2)

where ΔT is undercooling $T_m^0 - T_c$ when T_m^0 is equilibrium T_m, f is the factor expressed by $2T_c/(T_m^0 + T_c)$ that accounts
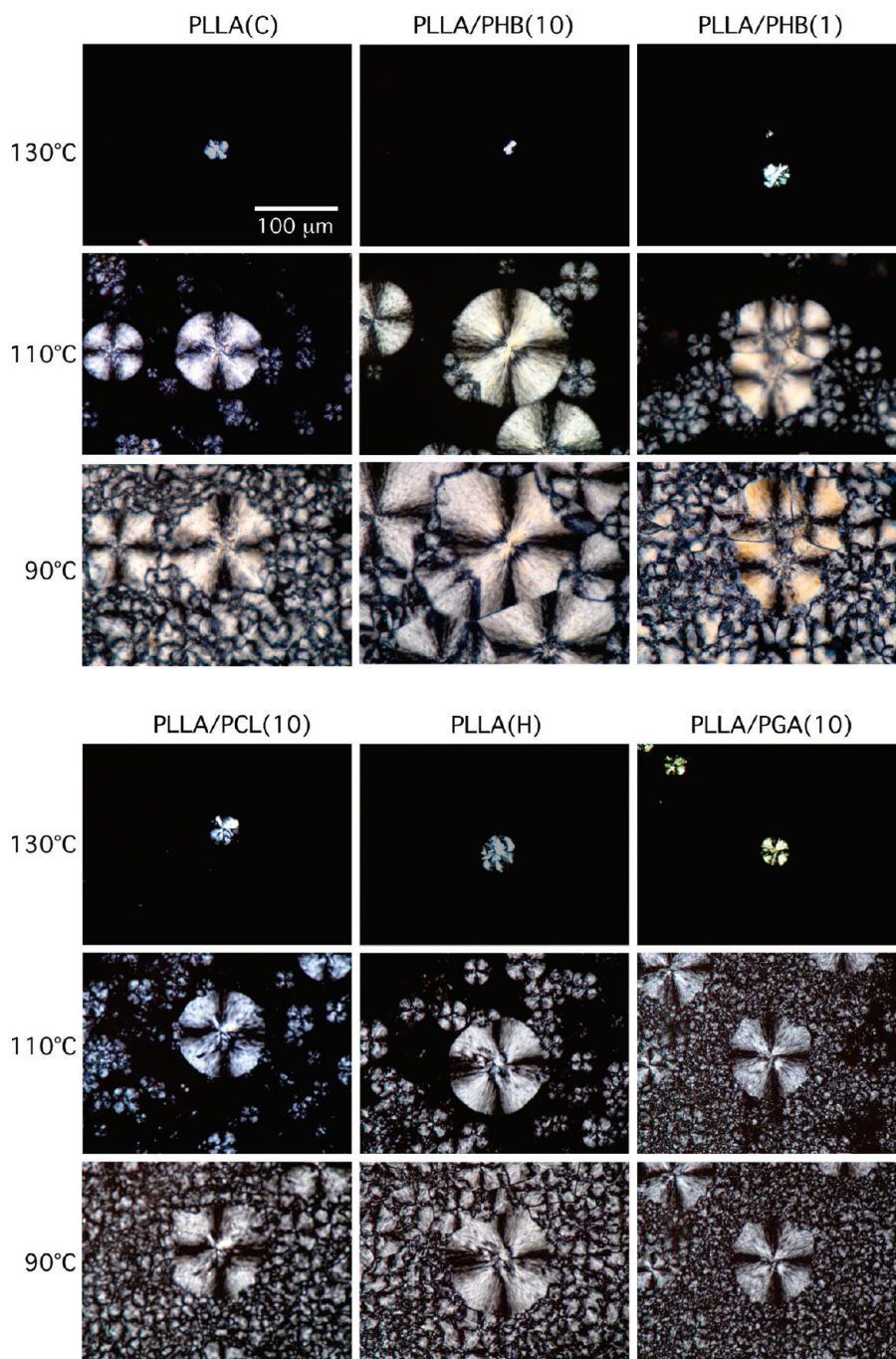
FIGURE 5. Polarized optical photomicrographs of pure PLLA and PLLA/PHB, PLLA/PCL, and PLLA/PGA blends taken during cooling from the melt (process II).

for the change in the heat of fusion as the temperature is decreased below T_m^0, U^* is the activation energy for the transportation of segments to the crystallization site, R is the gas constant, and T_∞ is the hypothetical temperature where all motion associated with viscous flow ceases. Figure 8 illustrates $\ln G + 1500/R(T_c - T_\infty)$ of pure PLLA and its blends as a function of $1/(T_c \Delta Tf)$, assuming that the blends are composed only of PLLA and T_m^0 is 212 °C (48). Here, we used the universal values of $U^* = 1500$ cal mol^{-1} and $T_\infty = T_g - 30$ K for comparison with the reported values (49−52). The plots in this figure give K_g as the slope and intercept ln G_0. The estimated K_g and G_0 values are summarized in Table

2. The data of pure PLLA and PLLA/PHB(10) and PLLA/PCL(10) blends are composed of two lines having different slopes. In these cases, we estimated the K_g and G_0 values for the two lines and assumed that the lines having high and low slopes were for regime III and II kinetics, respectively. On the other hand, the data of PLLA(H), PLLA/PHB(1), and PLLA/PGA(10) blends consist of one line. In these cases, regime II kinetics was expected from the K_g(II) values. The K_g(II) values of PLLA/PCL(10) (3.19×10^5 K^2), PLLA/PGA(10) (3.58×10^5 K^2), and PLLA/PHB(1) (2.97×10^5 K^2) blends are comparable to those of PLLA(C) and PLLA(H) (3.18×10^5 and 3.15×10^5 K^2) in the present study and the reported
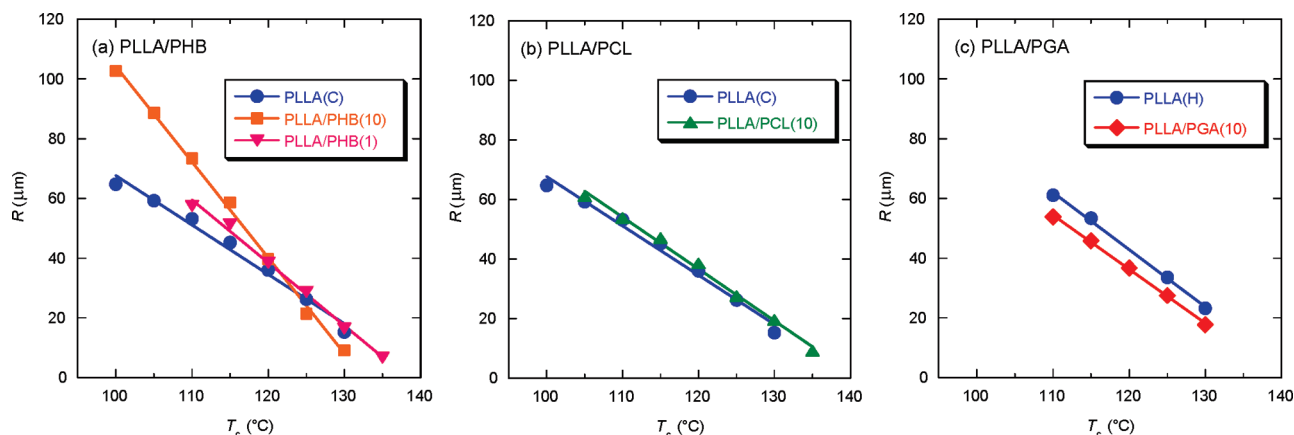
FIGURE 6. Radius (R) of spherulites in PLLA/PHB (a), PLLA/PCL (b), and PLLA/PGA(c) blends as a function of the crystallization temperature (T_c) (process II).

Table 2. Front Constant (G_0) and Nucleation Constant (K_g) for Pure PLLA and Its Blends (Process II)

incorporated polyester								
type	content (wt %)	casting solvent	$G_{av}{}^b$ (μm min^{-1})	T_{cc}(O)^b (°C)	G_0(II)^c (μm min^{-1})	G_0 (III)^c (μm min^{-1})	K_g (II)^c (K^2)	K_g (III)^c (K^2)
not added	0	C	1.66	141	1.32×10^8	5.89×10^{10}	3.18×10^5	5.26×10^5
		H	1.91	142	1.12×10^8		3.15×10^5	
PHB	10	C	3.20	133	2.17×10^{10}	2.90×10^{13}	4.67×10^5	7.18×10^5
PCL		C	1.74	141	1.61×10^8	1.07×10^{11}	3.19×10^5	5.35×10^5
PGA		H	1.81	140	4.39×10^8		3.58×10^5	
PHB	1	C	2.10	139	7.26×10^7		2.97×10^5	

^{a} C and H mean chloroform and HF2P, respectively. ^{b} G_{av} and T_{cc}(O) are the average G and onset temperature of cold crystallization for spherulite growth, which are estimated assuming that the spherulite growth takes place linearly with time irrespective of T_c. ^{c} (II) and (III) represent regimes II and III, respectively.
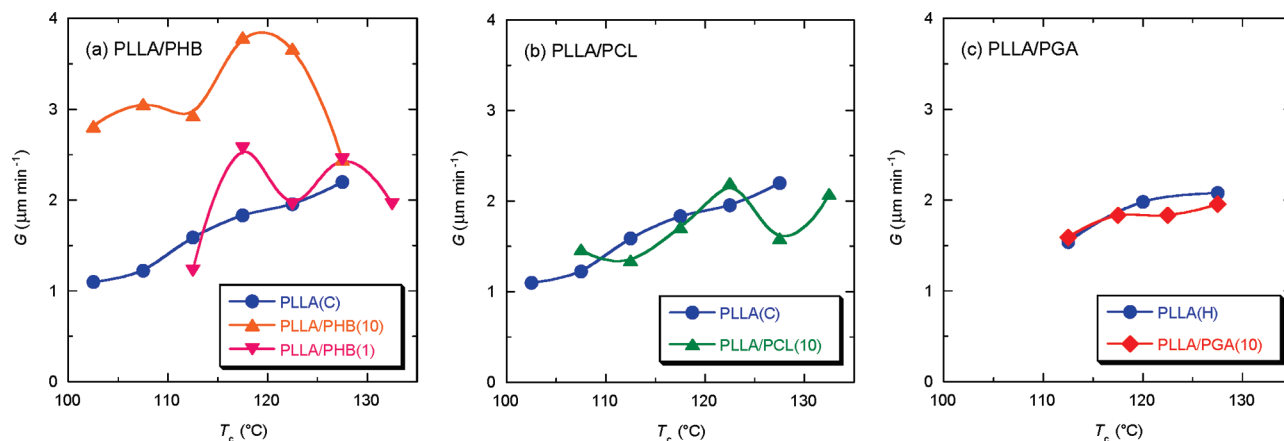

FIGURE 7. Radius growth rate of spherulites (G) in PLLA/PHB (a), PLLA/PCL (b), and PLLA/PGA (c) blends as a function of the crystallization temperature (T_c) (process II).

values ($2.20-2.55 \times 10^5$ K^2) (49−52), whereas the K_g(II) value of PLLA/PHB(10) (4.67×10^5 K^2) was much higher than that of pure PLLA and was close to the K_g(III) value of PLLA(C) (5.26×10^5 K^2) in the present study. We did not compare the obtained K_g(III) values with each other and the reported values because the some values were obtained from a small number of data points.

Avrami Analysis. The crystallinity relative to that after the completion of cold crystallization during heating and cooling (x_r) of PLLA was obtained from the DSC thermograms (Figures S1 and S2 in the Supporting Information) and

is plotted in Figures 9 and 10 as a function of T_c during DSC heating. x_r is defined as follows:

$$x_r = 100 \int_0^t (dH_{cc}/dt)\, dt \Big/ \int_0^\infty (dH_{cc}/dt)\, dt \qquad (3)$$

where dH_{cc} denotes the measured enthalpy of cold crystallization during an infinitesimal time interval dt. The crystallization behavior traced by DSC was analyzed with the Avrami theory. In the present study, we assume that the primary stage of nonisothermal crystallization can be de-
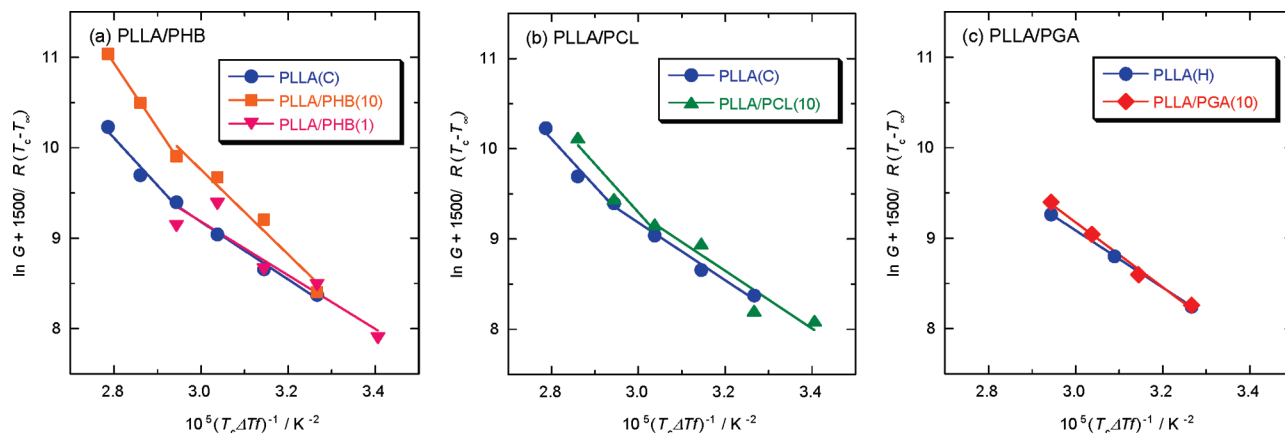
FIGURE 8. ln $G + 1500/R(T_c - T_\infty)$ of PLLA/PHB (a), PLLA/PCL (b), and PLLA/PGA (c) blends as a function of $1/(T_c \Delta Tf)$ (process II).
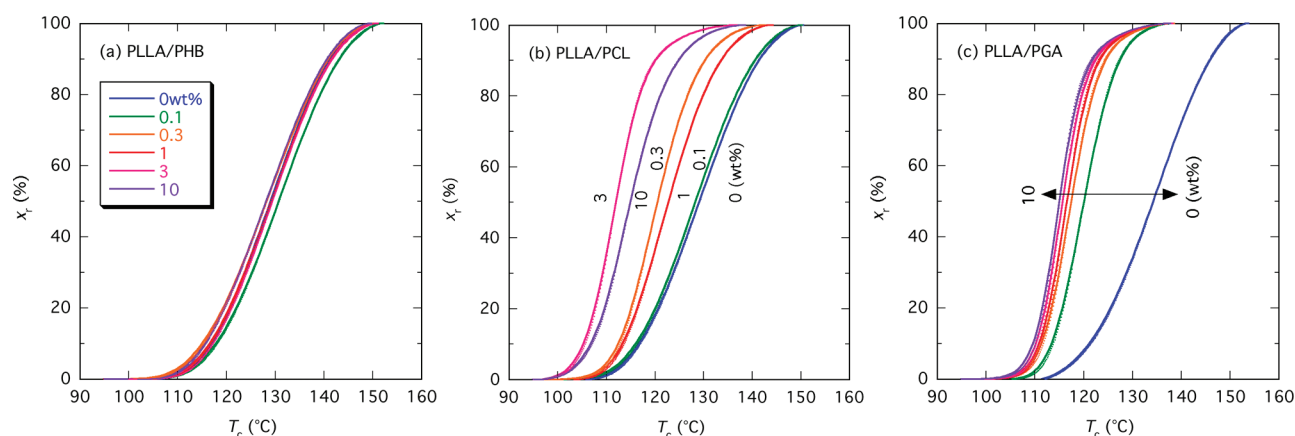

FIGURE 9. Crystallinity relative to X_c (x_r) of PLLA/PHB (a), PLLA/PCL (b), and PLLA/PGA (c) blends after the completion of crystallization as a function of the crystallization temperature (T_c) (process I).

scribed by the following Avrami equation, as suggested by Mandelkern (53−57):

$$1 - x_r/100 = \exp(-k_t t_c^n) \qquad (4)$$

where x_r (%) is the crystallinity relative to X_c after the completion of crystallization during heating or cooling, k_r is the nonisothermal crystallization rate constant, n is the Avrami exponent, and t_c is the crystallization time defined by the following equation:

$$t_c = |T_c - T_0|/\Phi \qquad (5)$$

where T_0 is T_c at which crystallization starts and Φ (K min^{-1}) is the heating or cooling rate. Figures 9 and 10 show x_r of pure PLLA and its blends during heating and cooling, respectively, as a function of T_c. For the calculation of t_c, T_0 values were fixed at 95 and 125 °C respectively for heating and cooling. Equation 4 can be transformed to eq 6:

$$\ln[-\ln(1 - x_r/100)] = \ln k_r + n \ln t_c \qquad (6)$$

To avoid deviation from the theoretical curves for x_r exceeding 25 %, as stated by Mandelkern (56), and the effect of a

relatively low S/N ratio at the initial stage of crystallization for x_r below 5 %, we used the data in the x_r range of 5−25 % to estimate n and ln k. The plots with eq 6 of pure PLLA and its blends during heating and cooling give n as the slope and intercept ln k_r (Figures S3 and S4 in the Supporting Information). The ln k_r values of nonisothermal crystallization can be corrected to ln k for isothermal crystallization by eq 7, as suggested by Jeziorny (57):

$$\ln k = (\ln k_r)/\Phi \qquad (7)$$

Also, the half-time ($t_{1/2}$) for PLLA crystallization was calculated by the following equation:

$$t_{1/2} = [(\ln 2)/k]^{1/n} \qquad (8)$$

The obtained n, k, and $t_{1/2}$ values are listed in Table 3 and Table S2 in the Supporting Information for heating and cooling. For heating from room temperature, the estimated n values for PLLA(C) and PLLA(H) were 4.8 and 5.1, respectively, and for cooling from the melt, they were 4.5 and 3.0, respectively.

For heating, the n values of PLLA/PGA blends (6.6−7.3) are much larger compared to 5.1 of pure PLLA(H), whereas those of PLLA/PHB and PLA/PCL blends (4.1−4.9 and
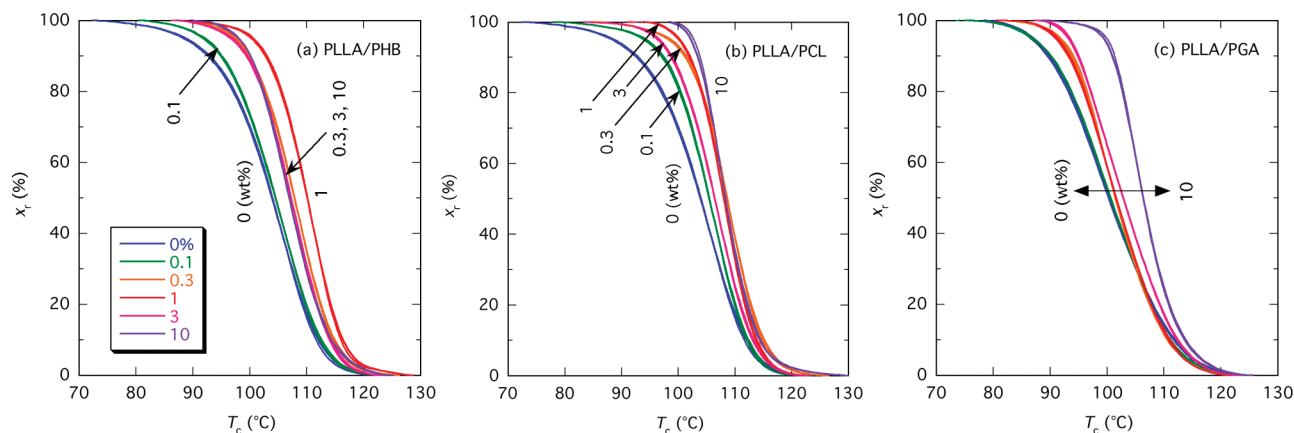
FIGURE 10. Crystallinity relative to X_c (x_r) of PLLA/PHB (a), PLLA/PCL (b), and PLLA/PGA (c) blends after the completion of crystallization as a function of the crystallization temperature (T_c) (process II).

Table 3. Avrami Exponent (n), Crystallization Rate Constant (k), and Half-Time ($t_{1/2}$) of Pure PLLA and Its Blends during Heating from Room Temperature (Process I) and Cooling from the Melt (Process II) (the Information for All Blends with Different Polyester Contents Is Shown in Table S2 of the *Supporting Information*)

crystallization procedure	incorporated polyester		casting solvent[a]	n	k (min^{-n})	$t_{1/2}$ (min)
	type	content (wt %)				
heating	not added	0	C	4.77	0.548	1.05
			H	5.13	0.484	1.07
	PHB	10	C	4.52	0.572	1.04
	PCL		C	3.50	0.750	0.98
	PGA		H	6.56	0.610	1.02
	PHB	1	C	4.68	0.553	1.05
cooling	not added	0	C	4.53	8.44×10^{-7}	20.2
			H	3.00	4.53×10^{-5}	24.8
	PHB	10	C	4.10	4.71×10^{-6}	18.2
	PCL		C	4.62	1.42×10^{-6}	17.0
	PGA		H	3.05	6.90×10^{-5}	20.5
	PHB	1	C	3.05	6.90×10^{-5}	20.5

[a] C and H mean chloroform and HF2P, respectively.

3.5−5.8, respectively) are similar to 4.8 of PLLA(C). Also, the n values of PLLA/PHB and PLLA/PCL blends (3.5−5.8) are comparable to ca. 4 of pure PLLA at $T_c = 110-132.5$ °C reported by Miyata and Masuko (44), whereas such high n values as for PLLA/PGA blends (6.6−7.3) have never been reported. The latter large values can be attributed to the high crystallite density due to the nucleating effect of PGA, which may have decreased the maximum x_r, below which the Avrami equation can be applied. For cooling from the melt, the estimated n values of PLLA/PGA blends were in the range of 3.1−4.0, whereas those of PLLA/PHB and PLA/PCL blends were in the ranges of 3.5−4.5 and 4.0−4.9, respectively. The n values of around 3 for PLLA/PGA blends are similar to those reported for pure PLLA (2.5−3.3 at $T_c = 90-130$ °C by Kolstad (58) and 2.8−3.2 at $T_c = 90-130$ °C by Iannace and Nicolais (59)). On the other hand, the n values of around 4 for PLLA/PHB and PLLA/PCL blends are comparable to those of PLLA at $T_c = 110-132.5$ °C reported by Miyata and Masuko (42). The differences in the reported n values of PLLA are attributable to the differences in the methods and procedures for monitoring the crystallinity (isothermal or nonisothermal), in the crystallization temperature range, and

in the relative crystallinity range used for the calculation. On the other hand, a large difference was observed for the n values of PLLA/PGA blends during heating and cooling, whereas a very small or insignificant difference was observed for the n values of PLLA/PHB or PLLA/PCL blends during heating and cooling.

The k and $t_{1/2}$ values of pure PLLA were affected by the solvent type, crystallization process (the direction and rate of temperature change), and temperature range. The dependence of $t_{1/2}$ values on the polyester type and content showed that, for both heating and cooling, PCL and PGA are effective crystallization-accelerating agents for PLLA. For heating, the k values of PLLA/PCL and PLLA/PGA blends increased with an increase in the PCL and PGA content, respectively, although those of PLLA/PHB blends were independent of the PHB content. For cooling, the k values of PLLA/PHB and PLLA/PCL blends gave a maximum at 0.3 wt %, whereas those of PLLA/PGA blends were highest at 10 wt %.

DISCUSSION

DSC and POM results indicated that three biodegradable polyesters, PHB, PCL, and PGA, can act as crystallization-

ACS APPLIED MATERIALS & INTERFACES

accelerating agents when their polymer contents are carefully selected. The final effects of an incorporated second polymer on PLLA crystallization can be classified as (1) the effect of increasing spherulite (or crystallite) nuclei per unit mass and (2) the effect of increasing G. These effects basically depend on the factors of (1) the miscibility of PLLA with the second polymer (or the dilution effect), (2) the direct nucleating ability or nucleation-assisting ability of the second polymer, which should be affected by the state of the second polymer (in the crystalline or in the noncrystalline state), and (3) the chain mobility of PLLA at T_c, which depends on the T_g value of the second polymer relative to that of PLLA. In a miscible or partially miscible system, the dilution effect of the second polymer will lower the driving force for the formation of crystalline nuclei and the second polymer can be a steric obstacle for the diffusion of PLLA chains to the crystallite growth sites or self-nucleating sites. This will delay the nucleation and growth of the crystallites (or spherulites). However, if PLLA is miscible with the second polymer, which has a T_g value lower than that of PLLA, the second polymer will increase the chain mobility of PLLA and, thereby, can assist the self-nucleation of PLLA and increase G. Therefore, the total effect of the second polymer is determined by the counterbalance between the two effects of disturbance and enhancement.

In the T_c range of PLLA (80−120 °C), PGA and PHB, the T_m values of which are respectively about 230 and 170 °C (36, 43), can crystallize, whereas PCL, the T_m value of which is about 60 °C (43), is in the melt. This means that only PHB and PGA can have a direct nucleating effect in the crystalline state. However, the very small changes in the $T_{cc}(S)$ values (Figures 1 and 3) and unchanged t_i values (Table S1 in the Supporting Information), as well as the unvaried $T_{cc}(O)$ (Table 1) of PLLA/PCL, PLLA/PHB, and PLLA/PGA blends, excluding the $T_{cc}(S)$ of PLLA/PGA(10) during heating and the lowered $T_{cc}(O)$ of PLLA/PHB(10) during cooling from the melt, indicate that the direct nucleating effect of these biodegradable polyesters was insignificant or very small because the normal direct nucleating agents, e.g., talc and the PLA stereocomplex, elevate $T_{cc}(S)$ of PLLA by 10 °C and more during cooling (18, 23, 32−35). Despite the unvaried $T_{cc}(O)$ during cooling, the final spherulite number per unit area of PLLA/PCL(10) and PLLA/PGA(10) blends was higher than those of PLLA(C) and PLLA(H) (Figure 5), the $T_{cc}(F)$ values of PLLA/PCL and PLLA/PHB, and PLLA/PGA blends during cooling were higher than those of pure PLLA, PLLA(C) and PLLA(H) (Figure 5), and the $T_{cc}(F)$ values of PLLA/PCL and PLLA/PGA blends (not PLLA/PHB bends) during heating were lower than those of pure PLLA, PLLA(C) and PLLA(H) (Figure 2). The $T_{cc}(S)$, $T_{cc}(P)$, $T_{cc}(F)$, and $T_{cc}(O)$ values of blends and of the area and size of PLLA spherulites in the blends strongly suggest that the nucleation-assisting effect is significant for PCL and PGA. On the other hand, the G values of PLLA/PHB(10) and PLLA/PHB(1) blends were respectively much and slightly higher than those of PLLA(C), whereas the G values of PLLA/PCL(10), PLLA/PGA(10), and PLLA/PHB(1) were comparable to those of PLLA(C) or PLLA(H)

(Figure 7). This is indicative of the fact that the effect of increasing G depends on the concentration of PHB. However, it should be noted that the incorporated PHB significantly decreased the spherulite number of PLLA per unit area. In summary, biodegradable polyesters are not nucleating agents but nucleating-assisting agents (PCL and PGA) and spherulite growth-accelerating agents (PHB).

The respective largely and slightly higher G values of PLLA/PHB(10) and PLLA/PHB(1) blends and the lower spherulite number per unit area of PLLA/PHB(10) compared to that of PLLA(C) can be explained as follows. That is, the relatively high miscibility of PLLA with PHB (39−41) and the lower T_g value of PHB (4 °C) (39, 40) compared to that of PLLA (56 °C) should have enhanced the chain mobility of PLLA, resulting in elevated G values. Moreover, the dilution effect of PHB lowered the nucleation of PLLA, leading to the lower spherulite number per unit area compared to that of pure PLLA. This effect should have decreased the elevating effect of $T_{cc}(F)$ for PLLA/PHB(10) during cooling compared to that for PLLA/PHB(1). However, in the present study, the decrease in the T_g value of blends was not traced because the amount of incorporated PHB was as low as 10 wt %. PCL has a T_g (ca. −60 °C) (60) much lower than that of PHB. However, the miscibility of PLLA with PCL is not as high as that with PHB (60). These facts can be the cause for no significant increase in the G values of PLLA even with the incorporation of 10 wt % PCL. For the same reason, in addition to the similar T_g values of PGA (about 35 °C) (61) and PLLA, the incorporated PGA had practically no significant effect on the G values of PLLA/PGA blends. Furthermore, the significantly higher $K_g(II)$ value of PLLA/PHB(10) compared to those of pure PLLA and PLLA/PCL(10) and PLLA/PGA(10) blends is indicative of the fact that the crystallization kinetics was altered by the presence of PHB when its content was increased to 10 wt %. This clarifies the high miscibility of PHB with PLLA in the present study compared to that of other biodegradable polyesters.

The large difference between the Avrami exponent n values of pure PLLA films [PLLA(C) and PLLA(H)] prepared with different casting solvents during cooling and the large difference between the n values of PLLA(H) during heating and cooling (Table 3) indicate that the effect of the solvent type on the nucleation and growth types of PLLA crystallites remained after the solvent evaporated and is larger for the cooling process and that the nucleation and growth types of crystallites in pure PLLA specimens prepared with HF2P are susceptible to the temperature-controlling direction (heating or cooling), rate, and temperature range. On the other hand, the n values of PLLA/PGA blends during heating were significantly higher than that of pure PLLA in the present study and in the reported literature. Therefore, the nucleation and growth types of PLLA crystallites varied only in the PLLA/PGA blends during heating, consistent with the results in Figures 1 and 3, and this shows that PGA is the most effective crystallization-accelerating agent. In contrast, the n values of PLLA/PHB and PLLA/PCL blends during heating and those of the three types of blends during cooling

were similar to those of pure PLLA in the present study and the reported literature (Table 3). In these cases, the incorporated polyesters did not affect the nucleation and growth types of PLLA crystallites.

Also, the large difference in the n values of PLLA/PGA blends during heating and cooling showed that the nucleation and growth types of PLLA crystallites were altered by the direction of the crystallization temperature change (heating or cooling), rate, and crystallization temperature range. In contrast, the very small or insignificant difference between the n values of PLLA/PHB and PLLA/PCL blends during heating and cooling means negligibly small effects of the direction of crystallization temperature change (heating or cooling), rate, and crystallization temperature range on the nucleation and growth types of PLLA crystallites. Finally, the different effect on PLLA crystallization during heating and cooling is partly attributable to the fact that different PLLA crystalline shapes (i.e., α and α') are formed at temperatures higher and lower than ca. 120 °C, respectively (62–64). Also, this may be the cause for the two slopes in Figure 8 and the different K_g values in Table 2.

CONCLUSIONS

Accelerated crystallization of PLLA took place in the presence of three biodegradable polyesters, and their effects, crystallization behavior, and rate depend on their type and content, crystallization conditions, and the type of solvent used for blend preparation. The accelerated crystallization of PLLA in the presence of biodegradable polyesters is attributable to the nucleation-assisting effect of PCL and PGA and the spherulite growth-accelerating effect of PHB, although the incorporated PHB lowered the spherulite number of PLLA per unit area. The spherulite growth-accelerating effect of PHB may have resulted from the relatively high miscibility of PLLA with PHB and the low T_g of PHB compared to that of PLLA. The crystallization kinetics of PLLA varied only in the case of PLLA/PHB blends during cooling from the melt, as evidenced by the K_g and G values. The nucleation and growth types of PLLA crystallites changed only in the case of PLLA/PGA blends during heating, as evidenced by the Avrami exponent n values.

Supporting Information Available: Radius growth rate of PLLA spherulites (G) and induction period for PLLA spherulite formation (t_i) for isothermal crystallization of pure PLLA and its blends (process III; Table S1; experiments were carried out with triplicate specimens for each data point), Avrami exponent (n), crystallization rate constant (k), and half-time ($t_{1/2}$) of PLLA with different contents of PHB, PCL, and PGA during heating from room temperature (process I) and cooling from the melt (process II) (Table S2), DSC thermograms of melt-quenched PLLA/PHB (a), PLLA/PCL (b), and PLLA/PGA (c) blends during heating from room temperature (process I; Figure S1), DSC thermograms of as-cast PLLA/PHB (a), PLLA/PCL (b), and PLLA/PGA (c) blends during cooling from the melt (process II; Figure S2), $-\ln(1 - x_r/100)$ of PLLA/PHB (a), PLLA/PCL (b), and PLLA/PGA (c) blends as a function of the crystallization time (t_c) (process I; Figure S3), $-\ln(1 - x_r/100)$ of PLLA/PHB (a), PLLA/PCL (b), and PLLA/PGA (c) blends as a function of the crystallization time (t_c) (process II; Figure S4). This material is available free of charge via the Internet at http://pubs.acs.org.

REFERENCES AND NOTES

(1) Kharas, G. B.; Sanchez-Riera, F.; Severson, D. K. In *Plastics from Microbes*; Mobley, D. P., Ed.; Hanser Publishers: New York, 1994; pp 93–137.

(2) Doi, Y., Fukuda, K., Eds. *Biodegradable Plastics and Polymers; Studies in Polymer Science 12*; Elsevier: Amsterdam, The Netherlands, 1994.

(3) Li, S.; Vert, M. In *Degradable Polymers. Principles and Applications*; Scott, G., Gilead, D., Eds.; Chapman & Hall: London, 1995; pp 43–87.

(4) Hartmann, M. H. In *Biopolymers from Renewable Resources*; Kaplan, D. L., Ed.; Springer: Berlin, 1998; pp 367–411.

(5) Ikada, Y.; Tsuji, H. *Macromol. Rapid Commun.* **2000**, *21*, 117–132.

(6) Garlotta, D. *J. Polym. Environ.* **2001**, *9*, 63–84.

(7) Albertsson, A.-C., Ed. *Degradable Aliphatic Polyesters (Advances in Polymer Science, vol. 157)*; Springer: Berlin, 2002.

(8) Södergård, A.; Stolt, M. *Prog. Polym. Sci.* **2002**, *27*, 1123–1163.

(9) Scott, G., Ed. *Biodegradable Polymers: Principles and Applications*, 2nd ed.; Kluwer Academic Publishers: Dordrecht, The Netherlands, 2002.

(10) Tsuji, H. In *Polyesters III; Biopolymers, vol. 4*; Doi, Y., Steinbüchel, A., Eds.; Wiley-VCH: Weinheim, Germany, 2002; pp 129–177.

(11) Auras, R.; Harte, B.; Selke, S. *Macromol. Biosci.* **2004**, *4*, 835–864.

(12) Slager, J.; Domb, A. J. *Adv. Drug Delivery Rev.* **2003**, *55*, 549–583.

(13) Tsuji, H. *Macromol. Biosci.* **2005**, *5*, 569–597.

(14) Gupta, A. P.; Kumar, V. *Eur. Polym. J.* **2007**, *43*, 4053–4074.

(15) Tsuji, H. *Degradation of Poly(lactide)-Based Biodegradable Materials*; Nova Science Publishers: New York, 2008.

(16) Thakur, K. A. M.; Kean, R. T.; Zupfer, J. M.; Buehler, N. U.; Doscotch, M. A.; Munson, E. J. *Macromolecules* **1996**, *29*, 8844–8851.

(17) Kolstad, J. J. *J. Appl. Polym. Sci.* **1996**, *62*, 1079–1091.

(18) Schmidt, S. C.; Hillmyer, M. A. *J. Polym. Sci., Part B: Polym. Phys.* **2001**, *39*, 300–313.

(19) Nam, J. Y.; Ray, S. S.; Okamoto, M. *Macromolecules* **2003**, *36*, 7126–7131.

(20) Pluta, M. *Polymer* **2004**, *45*, 8239–8251.

(21) Krikorian, V.; Pochan, D. J. *Macromolecules* **2005**, *38*, 6520–6527.

(22) Moon, S. I.; Jin, F.; Lee, C. J.; Tsutsumi, S.; Hyon, S. H. *Macromol. Symp.* **2005**, *224*, 287–296.

(23) Tsuji, H.; Takai, H.; Fukuda, N.; Takikawa, H. *Macromol. Mater. Eng.* **2006**, *291*, 325–335.

(24) Tsuji, H.; Kawashima, Y.; Takikawa, H. *J. Polym. Sci., Part B: Polym. Phys.* **2007**, *45*, 2167–2176.

(25) Liao, R.; Yang, B.; Yu, W.; Zhou, C. *J. Appl. Polym. Sci.* **2007**, *104*, 310–317.

(26) Pluta, M.; Murariu, M.; Ferreira, A. D. S.; Alexandre, M.; Galeski, A.; Dubois, P. *J. Polym. Sci., Part B: Polym. Phys.* **2007**, *45*, 2770–2780.

(27) Tsuji, H.; Kawashima, Y.; Takikawa, H.; Tanaka, S. *Polymer* **2007**, *48*, 4213–4225.

(28) Pan, P.; Zhu, B.; Dong, T.; Inoue, Y. *J. Polym. Sci., Part B: Polym. Phys.* **2008**, *46*, 2222–2233.

(29) Pan, P.; Liang, Z.; Cao, A.; Inoue, Y. *ACS Appl. Mater. Interfaces* **2009**, *1*, 402–411.

(30) Nam, J. Y.; Okamoto, M.; Okamoto, H.; Nakano, M.; Usuki, A.; Matsuda, M. *Polymer* **2006**, *47*, 1340–1347.

(31) Kawamoto, N.; Sakai, A.; Horikoshi, T.; Urushihara, T.; Tobita, E. *J. Appl. Polym. Sci.* **2007**, *103*, 198–203.

(32) Brochu, S.; Prud'homme, R. E.; Barakat, I.; Jérôme, R. *Macromolecules* **1995**, *28*, 5230–5239.

(33) Yamane, H.; Sasai, K. *Polymer* **2003**, *44*, 2569–2575.

(34) Anderson, K. S.; Hillmyer, M. A. *Polymer* **2006**, *47*, 2030–2035.

(35) Tsuji, H.; Takai, H.; Saha, S. K. *Polymer* **2006**, *47*, 3826–3837.

(36) Tsuji, H.; Tashiro, K.; Bouapao, L.; Narita, J. *Macromol. Mater. Eng. (Commun.)* **2008**, *293*, 947–951.

(37) Hiljanen-Vainio, M.; Varpomaa, P.; Seppälä, J.; Törmälä, P. *Macromol. Chem. Phys.* **1996**, *197*, 1503–1523.

(38) Tsuji, H.; Horikawa, G. *Polym. Int.* **2007**, *56*, 258–266, and references cited therein.

(39) Koyama, N.; Doi, Y. *Polymer* **1997**, *38*, 1589–1593.

(40) Hu, Y.; Sato, H.; Zhang, J.; Noda, I.; Ozaki, Y. *Polymer* **2008**, *49*, 4202–4210.

(41) Zhang, J.; Sato, H.; Furukawa, T.; Tsuji, H.; Noda, I.; Ozaki, Y. *J. Phys. Chem. B* **2006**, *110*, 24463–24471.

(42) Park, J. W.; Doi, Y.; Iwata, T. *Biomacromolecules* **2004**, *5*, 1557–1566.

(43) Tsuji, H.; Suzuyoshi, K. *Polym. Degrad. Stab.* **2002**, *75*, 347–355.

(44) Miyata, T.; Masuko, T. *Polymer* **1998**, *39*, 5515–5521.

(45) Di Lorenzo, M. L. *Polymer* **2001**, *42*, 9441–9446.

(46) Hoffman, J. D.; Frolen, L. J.; Ross, G. S.; Lauritzen, J. I., Jr. *J. Res. Natl. Bur. Stand., Sect. A* **1975**, *79A*, 671–699.

(47) Hoffman J. D.; Davis, G. T.; Lauritzen, J. I., Jr. In *Crystalline and Non-Crystalline Solids; Treatise on Solid State Chemistry, vol. 3*; Hannay, N. B., Ed.; Plenum: New York, 1976; Chapter 7, pp 497–614.

(48) Tsuji, H.; Ikada, Y. *Polymer* **1995**, *36*, 2709–2716.

(49) Vasanthakumari, R.; Pennings, A. J. *Polymer* **1983**, *24*, 175–179.

(50) Abe, H.; Kikkawa, Y.; Inoue, Y.; Doi, Y. *Biomacromolecules* **2001**, *2*, 1007–1014.

(51) Tsuji, H.; Miyase, T.; Tezuka, Y.; Saha, S. K. *Biomacromolecules* **2005**, *6*, 244–254.

(52) Tsuji, H.; Tezuka, Y.; Saha, S. K.; Suzuki, M.; Itsuno, S. *Polymer* **2005**, *46*, 4917–4927.

(53) Avrami, M. *J. Chem. Phys.* **1939**, *7*, 1103–1112.

(54) Avrami, M. *J. Chem. Phys.* **1940**, *8*, 212–224.

(55) Avrami, M. *J. Chem. Phys.* **1941**, *9*, 177–185.

(56) Mandelkern, L. *Crystallization of Polymers*; McGraw-Hill Book Co.: New York, 1964.

(57) Jeziorny, A. *Polymer* **1978**, *19*, 1142–1144.

(58) Kolstad, J. J. *J. Appl. Polym. Sci.* **1996**, *62*, 1079–1091.

(59) Iannace, S.; Nicolais, L. *J. Appl. Polym. Sci.* **1996**, *64*, 911–919.

(60) See for example: Tsuji, H.; Ikada, Y. *J. Appl. Polym. Sci.* **1998**, *67*, 405–415.

(61) Perrin, D. E.; English, J. P. In *Handbook of Biodegradable Polymers; Drug Targeting and Delivery, vol. 7*; Domb, A. J., Kost, J., Wiseman, D. M., Eds.; Harwood Academic Publishers: Amsterdam, The Netherlands, 1997; Chapter 1, pp 3–27.

(62) Pan, P.; Zhu, B.; Kai, W.; Dong, T.; Inoue, Y. *J. Appl. Polym. Sci.* **2008**, *107*, 54–62.

(63) Kawai, T.; Rahma, N.; Matsuba, G.; Nishida, K.; Kanaya, T.; Nakano, M.; Okamoto, H.; Kawada, J.; Usuki, A.; Honma, N.; Nakajima, K.; Matsuda, M. *Macromolecules* **2007**, *40*, 9463–9469.

(64) Zhang, J.; Tashiro, K.; Tsuji, H.; Domb, A. J. *Macromolecules* **2007**, *40*, 1049–1054.

AM9002759